Arabian Journal of Geosciences (2022) 15: 506
https://doi.org/10.1007/s12517-022-09781-1

ORIGINAL PAPER

Geotechnical database building and 3D modeling of the soil in Medina, Saudi Arabia

Alaa A. Masoud[1] · Ahmed M. Saad[2] · Osama N. H. El Shafaey[3]

Received: 3 September 2020 / Accepted: 23 February 2022 / Published online: 10 March 2022

Abstract

Sustainable innovative uses of underground space dictate the use of efficient and cost-effective techniques for geo-investigation and planning. This is now affordable with detailed three-dimensional (3D) geotechnical models of the soil properties that provide key source data to tackle the inherent complex nature of the subsurface beneath the densely urbanized cities. These models are vital for the sustainable cities safe urban expansion, tunneling, and optimal design of settlements. In the present research, 3D models were built using 189 samples collected from 92 boreholes distributed in Medina, Saudi Arabia. Models built included the database generated for soil varieties, classes of cohessionless, and cohesive soils based on their standard penetration test (SPT)-N value, along with rock quality designation (RQD) of the sound bedrocks, soil classes according to AASHTO, grain size analysis, Atterberg limits (liquid limits and plasticity index), the shear stress parameters (friction angle, Ø, and cohesion, *c*), the unconfined compression strength, and the soil water chemistry (pH, $SO3^{2-}$, and Cl^{-}). Five soil varieties that were recognized ranged in size from clays to cobbles overlain by fills and underlain by basalt, rhyolite/granite, or andesite. AASHTO main soil types are A-1-b, A-2–4, and A-1-a. Out of the 189 samples, 174 were non-plastic while 15 samples showed an average liquid limit of 42.57% and plasticity index average of 9.92. Friction angle averaged 30.47° with *c* values average of 0.11. Unconfined compressive stress averaged 609 kg/cm^2. Soil water chemistry clarified alkaline water (8–8.6 pH) with means of 0.1 for Cl^{-} and $SO3^{2-}$ contents. Geotechnical properties are spatially rendered in 3D and interpreted to better enable city planners predict and locate risk zones in the urban underground space.

Keywords Geotechnical 3D models · Stochastic models · Rock quality designation · Medina · Saudi Arabia

Introduction

Rapidly growing cities with high anthropogenic pressure commonly face extensive infrastructural development in their land use planning while minimizing environmental impact and providing long-term sustainability. The subsurface soil conditions have become essential to support safe design of buildings, railway lines, pipelines, tunnels, bridges, dams, and roads. Geotechnical properties of soils influence the stability and economical design of structures and deemed necessary in the design of foundation, road pavement, retaining structures, and utilities to be safe, serviceable, sustainable, and economic for future construction projects.

City-scale 3D models are of great importance in all stages of a construction and help improve the planning and storing of the soil information data in databases for future use. This requires in-depth knowledge based on a comprehensive database of the soils upon which cities were built (Kolat et al. 2006, 2012; Donghee et al. 2012; Price, et al. 2018; He, et al. 2020) to assess soil suitability to meet planned uses and manage the proper design and construction, and also to avoid future risks at an early stage of design. This can also help prevent adverse environmental impact or structural failure and prevention of post construction problems.

Sound reliable geotechnical data is indispensible to achieve accurate site investigation formed commonly of a

Responsible editor: Zeynal Abiddin Erguler

✉ Alaa A. Masoud
alaa_masoud@science.tanta.edu.eg

[1] Remote Sensing Laboratory, Geology Department, Faculty of Science, Tanta University, Tanta 31527, Egypt

[2] Geology Department, Faculty of Science, Al-Azhar University, Cairo, Egypt

[3] Omar Jazzar Consulting Engineers Office, Branch of Qassim, Hail, and Madinah, Saudi Arabia, Saudi Arabia

combination of in situ testing, site description, ancillary data, and soil and rock sampling for further laboratory tests. Soil data measurements are usually spaced to minimize cost of borehole drilling where appropriate interpolation techniques are applied to fill the area between the widely spaced data points. These can help anticipate unforeseen soil characteristics not only for design and economy but also for construction techniques. Unraveling the accurate soil spatial geotechnical variability is imperative in optimum cost, time, and safety and efficient setting of hazard mitigation measures that can play a decisive role to help efficient land suitability prioritization and land use management for future urban expansion projects (e.g., Das 2005; CGS 2006; Hack et al. 2006; De Rienzo, et al. 2008; Kolat, et al. 2012; Masoud 2015; Masoud, et al. 2016). This urges the use of a multidisciplinary and 3D modeling approach that can integrate the multivariate statistical and the geostatistical techniques.

The 3D modeling approach is commonly influenced by the spatial variability of soils that naturally results from many disparate sources dependent on nexus of factors related to the geological and hydrogeological conditions, prevailing seasonal temperature changes, wind, rainfall, and human practices (Chang et al. 2005; Phien-wej et al. 2006; Chrétien et al. 2007) which may lead to severe geotechnical problems in the 3D space. In the desert regions, wadi deposits are underlain by beds of hard rocks at various depths. This type of soil presents many problems during construction due to its high permeability and particularly arises where sound rock bed underlies the soil. Collapse of soil structure often takes place under prolonged exposure to moisture.

The 3D models are widely rendered in two forms: layers on the top and base boundaries in the form of borehole and as stochastic probabilistic models of regular shapes of volume elements (voxels) representing the interpolated properties (e.g., grain size, density, shear strength parameters, etc.) at and in-between the sampling points in the 3D space. Stochastic models are quantitative and objective, based on statistical probability of occurrence of a given layer or a specified physical property. Such deterministic models have been proven to be widely applicable to modeling of many single-solution environmental and geotechnical problems (Aldiss et al. 2012) of the shallow subsurface (< 100 m below ground level) formed mostly of the engineering soils or weak rocks where complexity related to geologic discontinuity structures is low.

The provision of geotechnical database in 3D is a central requirement of mainstreaming into a city's master plan to optimize the soil use which is lacking in the literature and uncommon in desert regions. Therefore, in this research, the 3D modeling was appraised to improve the geotechnical investigations and the distribution of the measured soil properties and to tackle the inherent complex nature in the un-sampled areas. The prime objective is to locate and map the geotechnically at-risk areas to mitigate hazards by focusing future sustainable development plans to inform pre-development design and construction and to take suitable ameliorative and preventive measures. This will greatly intensify fairly accurate and economical geotechnical design since the cost of data collection, analysis, and mapping will be reduced using less dense boreholes.

Data and methods

Geotechnical data from ninety-two boreholes unevenly spatially distributed in the city with 189 soil samples were analyzed. Borehole index data recording names, geographic coordinates, elevation, soil layer types, and boundaries along with the depth of sampling data points and recorded corresponding properties are recorded in excel sheet. Models are built for the soil type variation, density classes of cohesive and cohessionless soils, rock quality designation (RQD), unconfined compression strength, shear stress parameters (Ø and *c*), Atterberg limits of plasticity, grain size analysis, and soil water chemistry. Spatial distribution of the geotechnical properties is rendered in Voxler 3 software. For the sake of visual clarity, the depth dimension is exaggerated 100 times in representing borehole log and 200 times for point data. Borehole coordinates were recorded and represented using the Universal Transverse Mercator (UTM) zone 37.

Standards of the American Society for Testing and Materials (ASTM) were applied for Sieve Analysis of Fine and Coarse Aggregates (C 136–96a); Liquid Limit, Plastic Limit, and Plasticity Index (ASTM D 4318–98); Maximum Index Density and Unit Weight Using a Vibratory Table (D 4253–00); Moisture Density Relationship (D 1557 Method "C"); Specific Gravity and Water Absorption of Aggregate (C 127–88); Direct Shear Test for Soils Under Consolidated Drained Conditions (D 3080–98); and unconfined compression strength (ASTM D 2166).

Relative soil density is indicated by the Standard Penetration Test (SPT)-N value, the number of blows required to affect the last 300-mm penetration below the seating drive. In this test, a split spoon sampler (50 mm diameter) was driven 450 mm into the soil with a hammer (63.5 kg) falling freely a distance of 760 mm. The sampler was driven in two stages: the initial 150-mm penetration of the sampler (seating drive) and the last 300-mm penetration (test drive).

The 3D models are rendered as soil layer boundaries and their corresponding relative density and the underlying RQD parameters of rocks, as well as stochastic probabilistic models of voxels for the interpolated properties in the 3D space. Stochastic models are rendered as points, iso-surfaces of equal values from two opposite viewing directions, and as volumetric solid models.

Study area

The holy city of Medina was chosen, guided by the city's master plan. This plan identifies environmental and sustainability goals as part of a series of planning measures to achieve the safe and efficient use of land. The prime objective is to provide the 3D spatial assessment of the soil geotechnical variability that contribute to the successful implementation of the future safe urban expansion plan that comprise mixed retail, residential, education, commercial, open space, and subsurface basement construction for car parking. The city is nearly flat elevated at 600–610 m surrounded by low to medium altitude hills/mountains (900–1100 m) and lava plateaus (620–750 m) with a gentle

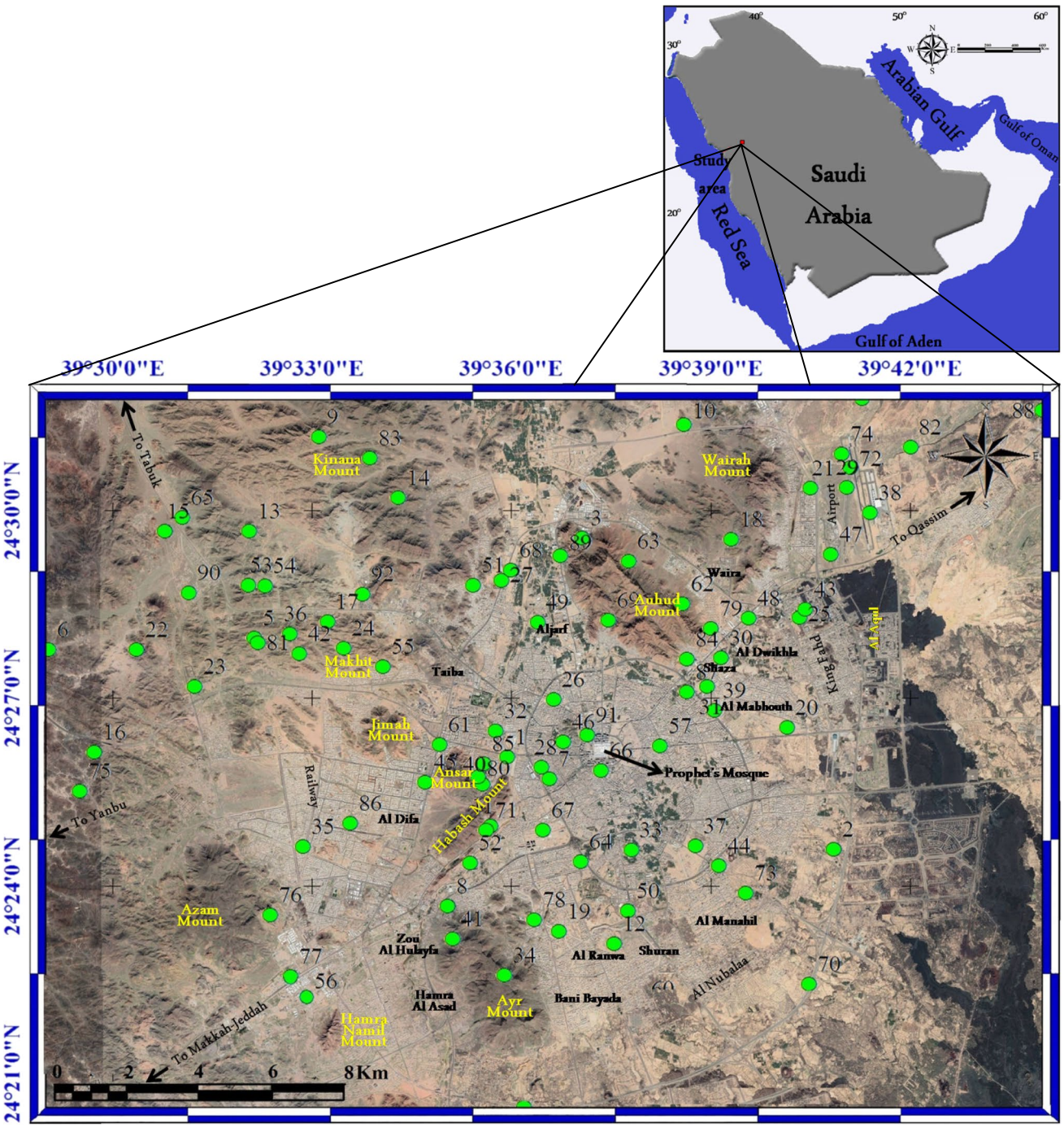

Fig. 1 Location map and borehole distribution (Google Earth 2019)

northwest slope. The most famous among these mountains are Uhud in the north and Ayr in the southwest (Fig. 1).

The city is located in the western part of the Precambrian Arabian Shield overlaid by lava plateaus (i.e., harrats) and sediments from the Tertiary and Quaternary ages. The area is covered by veneer of Wadi deposits composed of sand, gravels, and silt inter-bedded with clay that carry water for a few days, but most water is lost through direct infiltration and evaporation. Most of the groundwater wells are located in the basaltic aquifer to the east of wadi Aqiq. Water table in the area ranges from 50 to 80 m below the surface (Al-Shaibani, et al. 2007).

Geologically (Fig. 2), the upper Proterozoic rocks intrude the wadi deposits and compose mainly of mafic to silicic

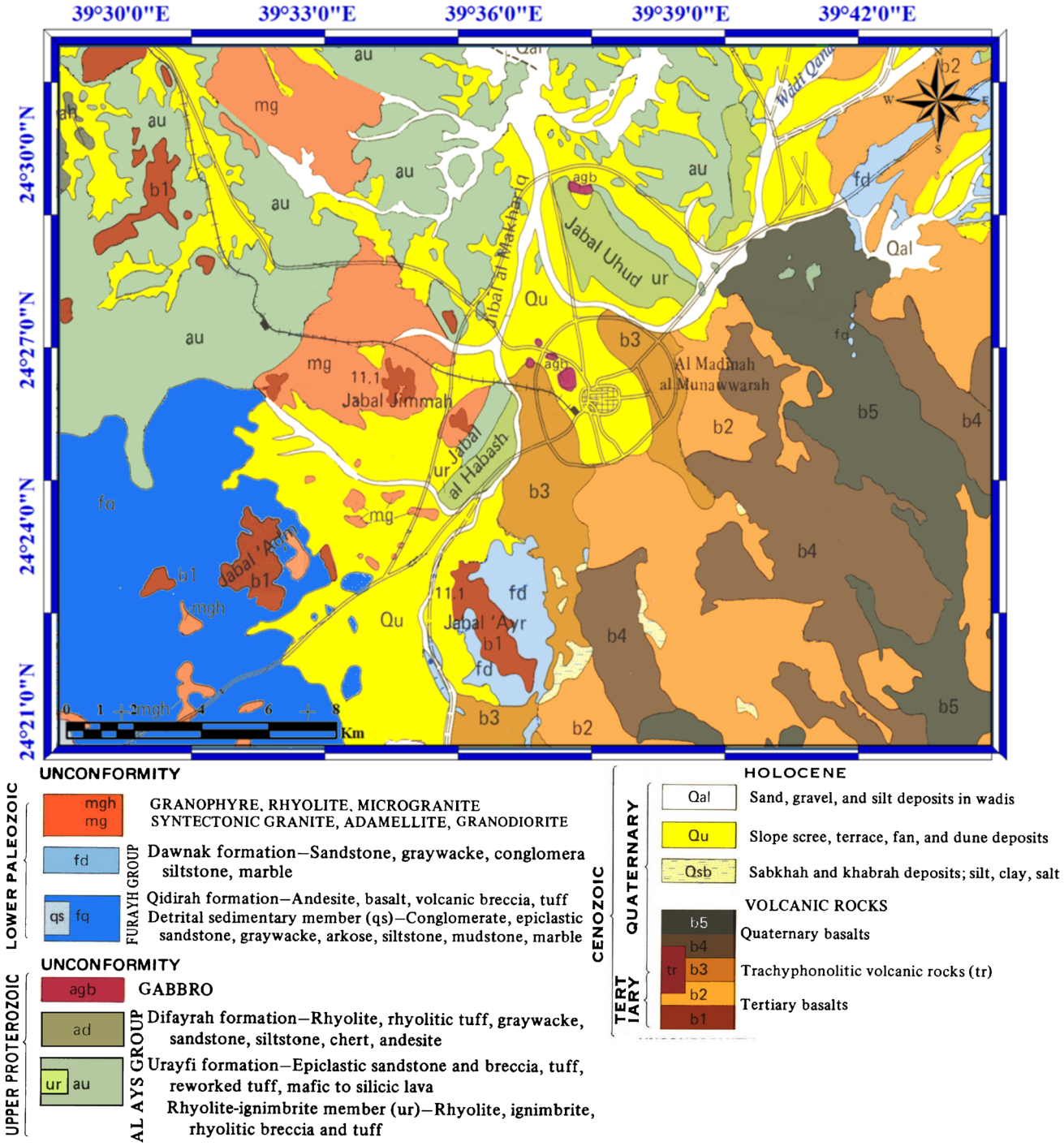

Fig. 2 Geological map of the study area (Modified after Pellaton 1981)

Table 1 Descriptive statistics of soil properties

	Grain sizes (%)			Atterberg limits		Shear strength		UCS kg cm^{-2}	Soil water chemistry		
	Gravel	Sand	Fines	LL%	PI	*C*	*Ø*	UCS	pH	Cl^-	SO_3^{2-}
Min	0	6.7	1.3	22.9	3.75	0.01	27	0	8	0.016	0.012
Max	78.5	88.7	93.3	71.3	19.5	0.41	35	1462.29	8.6	0.41	0.45
Mean	31.8	45.20	23.55	42.57	9.92	0.11	30.47	609.52	8.07	0.10	0.11
StDev	19.26	17.68	18.97	15.77	5.00	0.10	2.01	287.78	0.10	0.10	0.09
Count	128	128	128	15	15	77	77	67	98	98	98

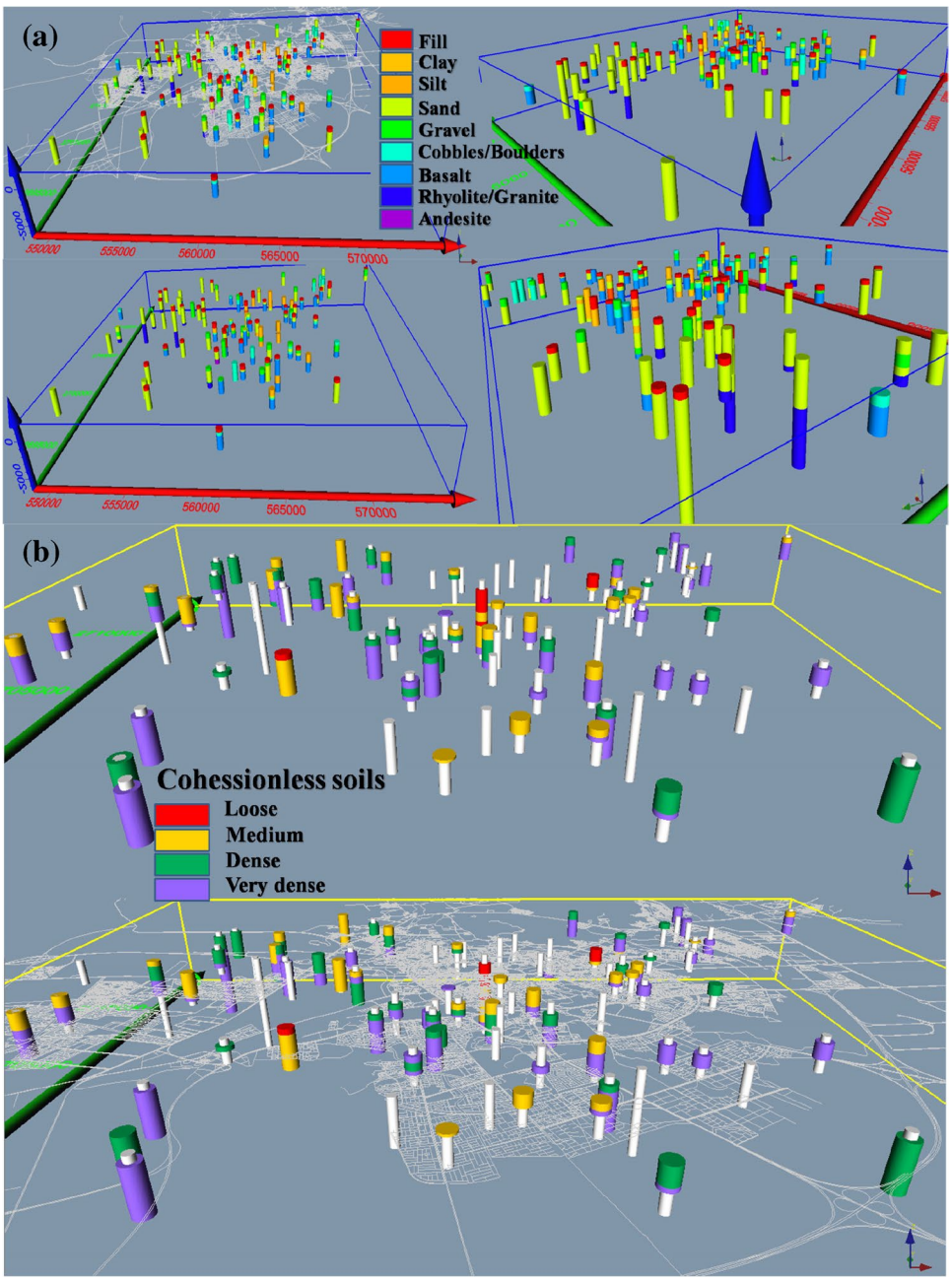

Fig. 3 Three-dimensional models of **a** the soil types and **b** their classification according to SPT of the cohessionless/**c** cohesive soils and **d** the RQD of bedrocks

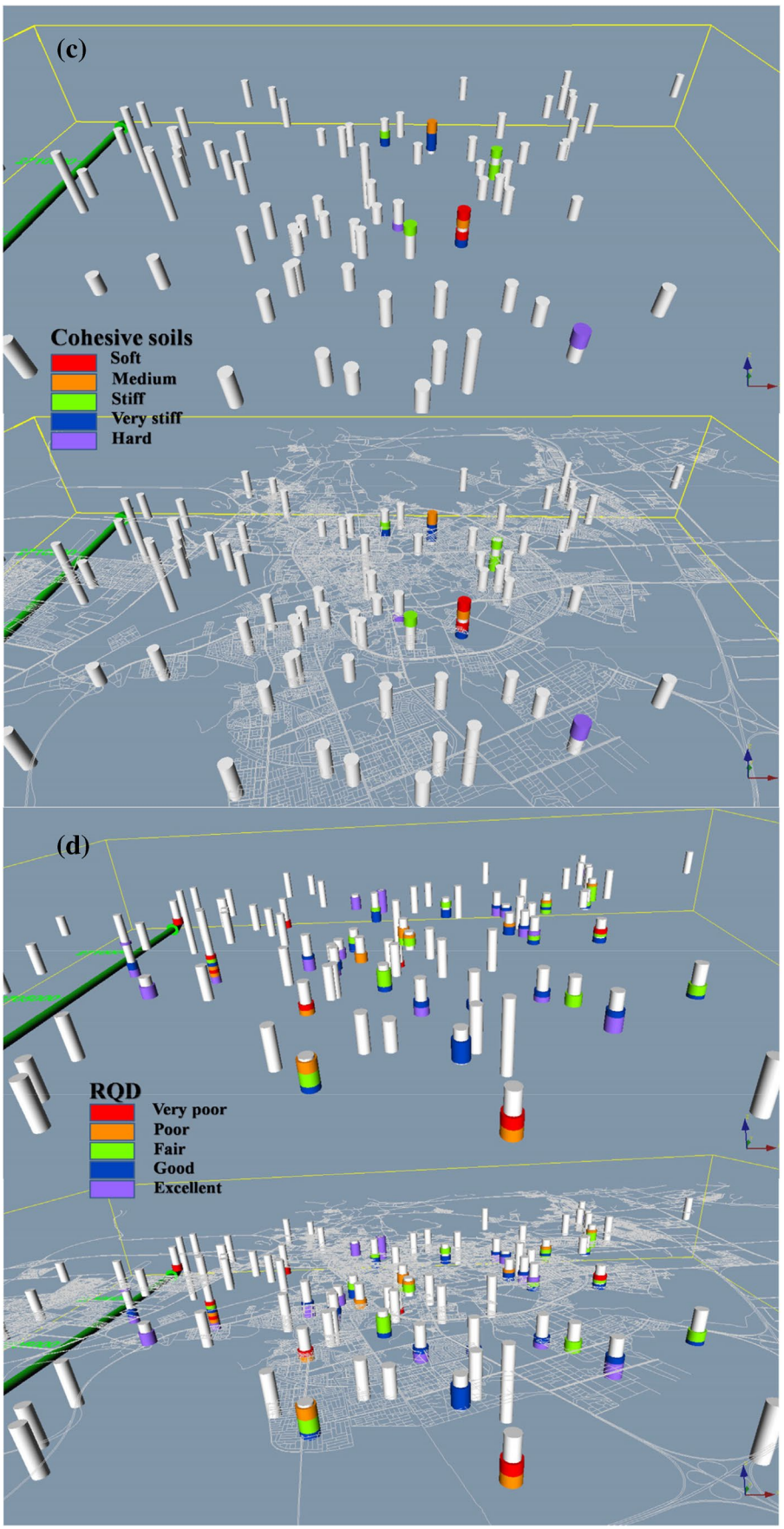

Fig. 3 (continued)

Table 2 Description of the monitored soil varieties with classes for the cohessionless and cohesive soils and the rock RQD

Soil variety		Description	Thickness (m)	Measured	%	Cohesionless soils	Cohesive soils	RQD
Fill	**Min**	Light to dark brown, non-plastic, silty sand intermixed with gravel/boulders, and debris	0.5			Dense		Excellent
	Max		4.5			Loose		Excellent
	Count		44	9	20.5			
Clay	**Min**	Grayish brown silty clay	1.5			Loose	Stiff	
	Max		6			Loose	Stiff	
	Count		2	1	50			
Silt	**Min**	Light brown, grayish, yellowish, sandy silt	0.5			V. Dense	Hard	
	Max		7.5			Loose	Soft	
	Count		33	31	93.9			
Sand	**Min**	Light gray, light to Greyish brown, dark brown, greenish brown, plastic to non-plastic, well to poorly graded clayey to silty sand, and sand with silt, gravel and/or cobbles	0.5			V. Dense		Fair
	Max		12.5			Medium		Fair
	Count		109	92	84.40			
Gravel	**Min**	Light gray, light to greyish brown, dark brown, greenish brown, plastic to non-plastic, well to poorly graded silty to sandy gravel, with silt, sand, and/or cobbles	0.5			V. Dense		
	Max		8.5			Medium		
	Count		41	37	90.2			
Cobbles	**Min**	Grey to dark grey, cobbles and boulders of vesicular basalt intermixed with sandy silt, silty sand, silty gravel, and gravel	0.5			V. Dense		V. poor
	Max		10			Dense		V. poor
	Count		27	10	35.71			
Basalt	**Min**	Light to dark grey, fine grained, of varying degrees of hardness, weathering, and fracturing, vesicular basalt bedrock	0.5					Excellent
	Max		9					V. poor
	Count		88	69	78.4			
Rhyolite/ Granite	**Min**	Greenish gray, grayish to reddish brown, and pink, of varying degrees of hardness, weathering, and fracturing, rhyolite/ granite bedrock	1					Excellent
	Max		6					V. poor
	Count		20	14	70			
Andesite	**Min**	Greenish grey moderately hard, highly to intensely fractured Andesite bedrock	1					
	Max		1.5					Poor
	Count		2	2	100			V. poor

volcanic rock (e.g., Uhud Mountain) and derivative epiclastic and detrital sedimentary rock (Pellaton, 1981). The Al Ays Group is generally intruded by younger igneous intrusions including layered gabbro complex, granite batholiths, granodiorite and diorite, and isolated gabbro stocks. Tertiary and Quaternary basalt lava fields (known as Harrats) formed at the same time as the Red Sea rifting (Camp and Roobol 1991) composed of alkali olivine basalt typically derived from rift volcanism. Quaternary deposits in the study area comprise surficial deposits of varied fluvial, aeolian, and lacustrine origin and are commonly closely intermixed. Wadi alluvium of gravel, sand, and clay, these deposits follow the present-day drainage pattern.

Okasha and Abduljauwad (1992) reported that construction work carried out in the clayey soils of Al-Medinah city, in particular the greenish-brown clays, has met many problems. The soils are composed of quartz, feldspar, smectite, calcite, kaolinite, and some chlorite and were highly expansive indicated from Atterberg limits, clay fractions as well as from the axial free swelling, percentage of swell, and swelling procedure.

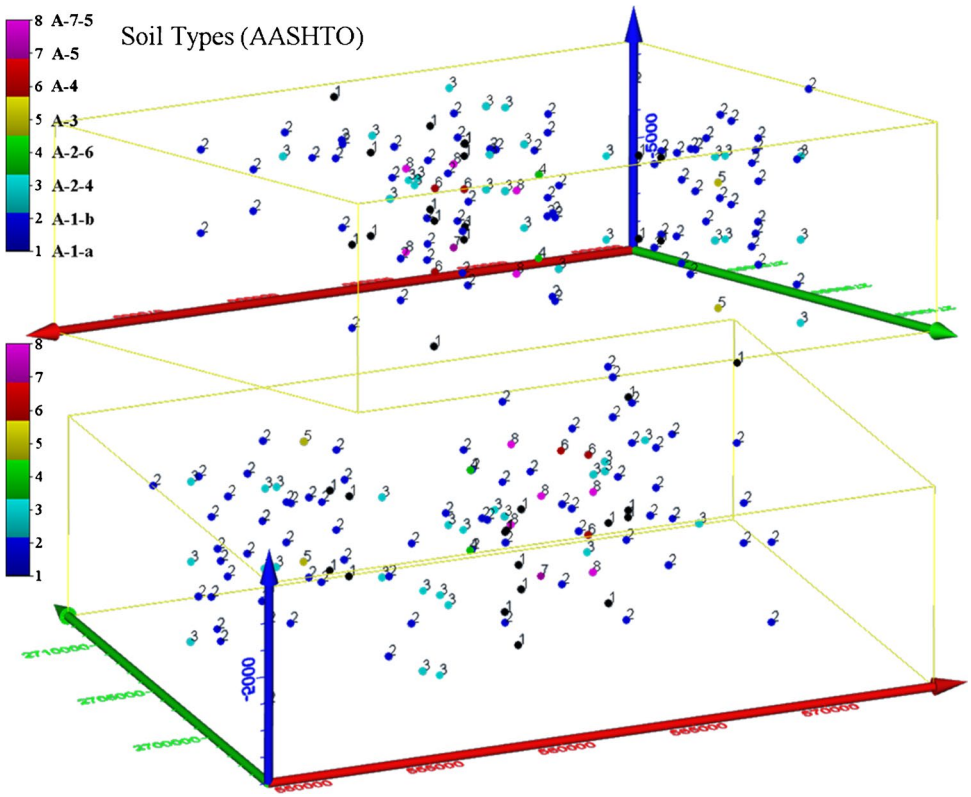

Fig. 4 Soil types according to AASHTO classification

Results

Soil descriptive statistics

Descriptive statistics of the city soil parameters of grain sizes, Atterberg limits, direct shear stress parameters (friction angle Ø and cohesion *c*), unconfined compression strength, and soil water chemistry (pH, Cl^-, and SO_3^-) are shown in Table 1. Borehole total depth varied between 8 and 30 m from the ground surface. Grain size distribution of 128 samples indicated the dominance of the average content of sand (45.20%) followed by gravel (31.8%) and fines (23.55%). Out of the 189 samples, 174 were non-plastic while 15 samples showed an average liquid limit (LL) of 42.57% (22.9–71.3% range) and plasticity index average of 9.92 (3.75–19.5 range). Friction angle of shear test showed an average of 30.47° (27°–35° range) with cohesion, *c*, values averaged 0.11 (0.01 to 0.41 range) indicating the dominance of the cohessionless soils. Unconfined compressive stress averaged 609 kg cm^{-2} (0–1462 kg cm^{-2}). Soil water chemistry clarified alkaline water (8–8.6 pH) with means of 0.1 for Cl^- and SO_3^{2-} contents. According to AASHTO classification, 56.5% showed A-1-b type, 19.5% A-2–4, 14% A-1-a, and 10% varied between A-7–5, A-4, A-2–6, A-3, and A-5.

Soil varieties and AASHTO types

Three-dimensional models of the soil varieties are shown on Fig. 3a. Cohessionless and cohesive soil classes according to their SPT soils are shown on Fig. 3b and c. Bedrocks of basalt, rhyolite/granite, and andesite and their relative strength classified according to their corresponding RQD% are shown on Fig. 3d. The main five soil varieties that are recognized ranged in size from clays to cobbles overlain by fills and underlain by basalt, rhyolite/granite, or andesite (Table 2).

The cohessionless soil contains little to no clay or fine particles while cohesive soils contain high amounts of clay and fine particles. Cohesive soils are those in which the surface forces of the soil particles are largely responsible for the soil strength (Scott 1963). Cohesive soils with clay and fine particular materials maintain a certain binding capacity that works to retain a soil's shape and consistency. Cohessionless soils consist of large or irregular-sized soil particles with little to no clay content and tend to shift or change in consistency under different environmental conditions such as in rain and wind conditions commonly associated with water infiltration and evaporation.

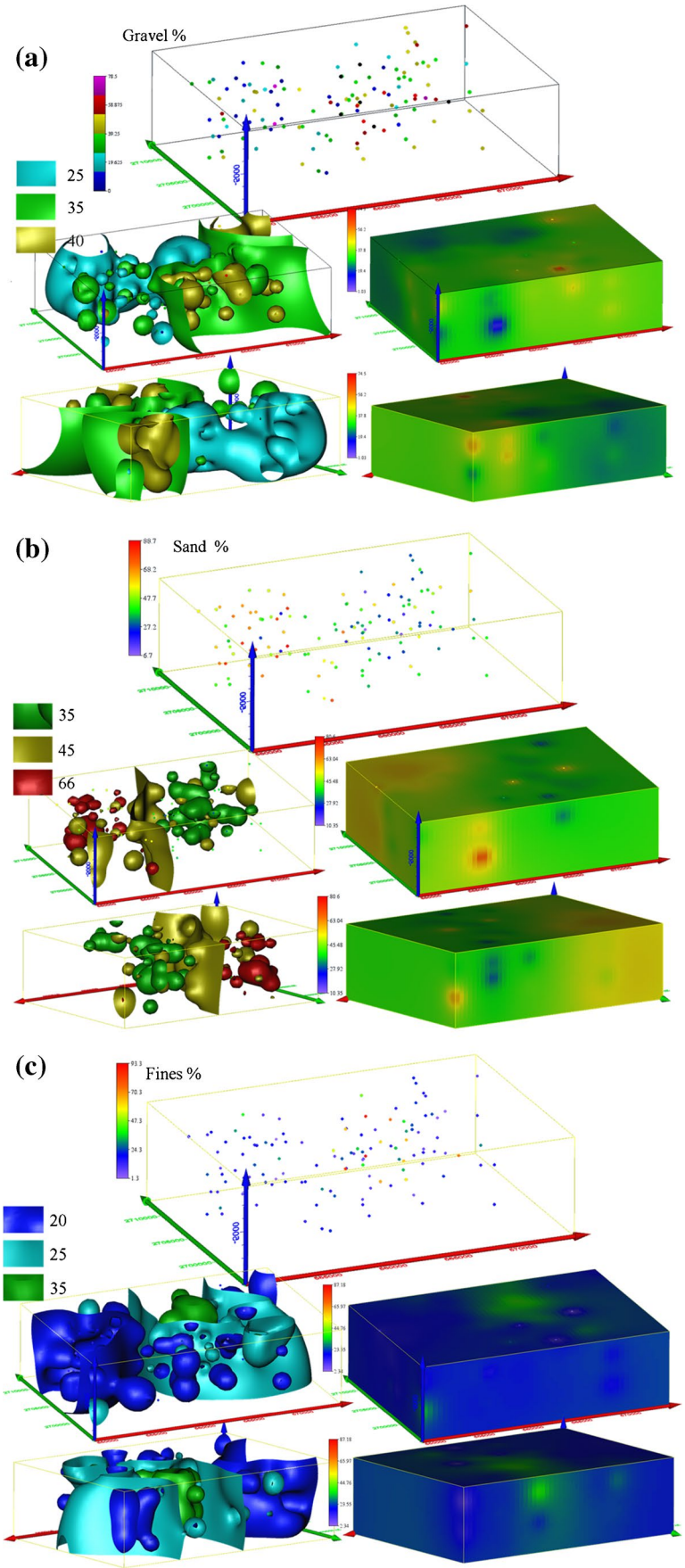

Fig. 5 Grain size distribution 3D models of the **a** gravel, **b** sand, and **c** fines

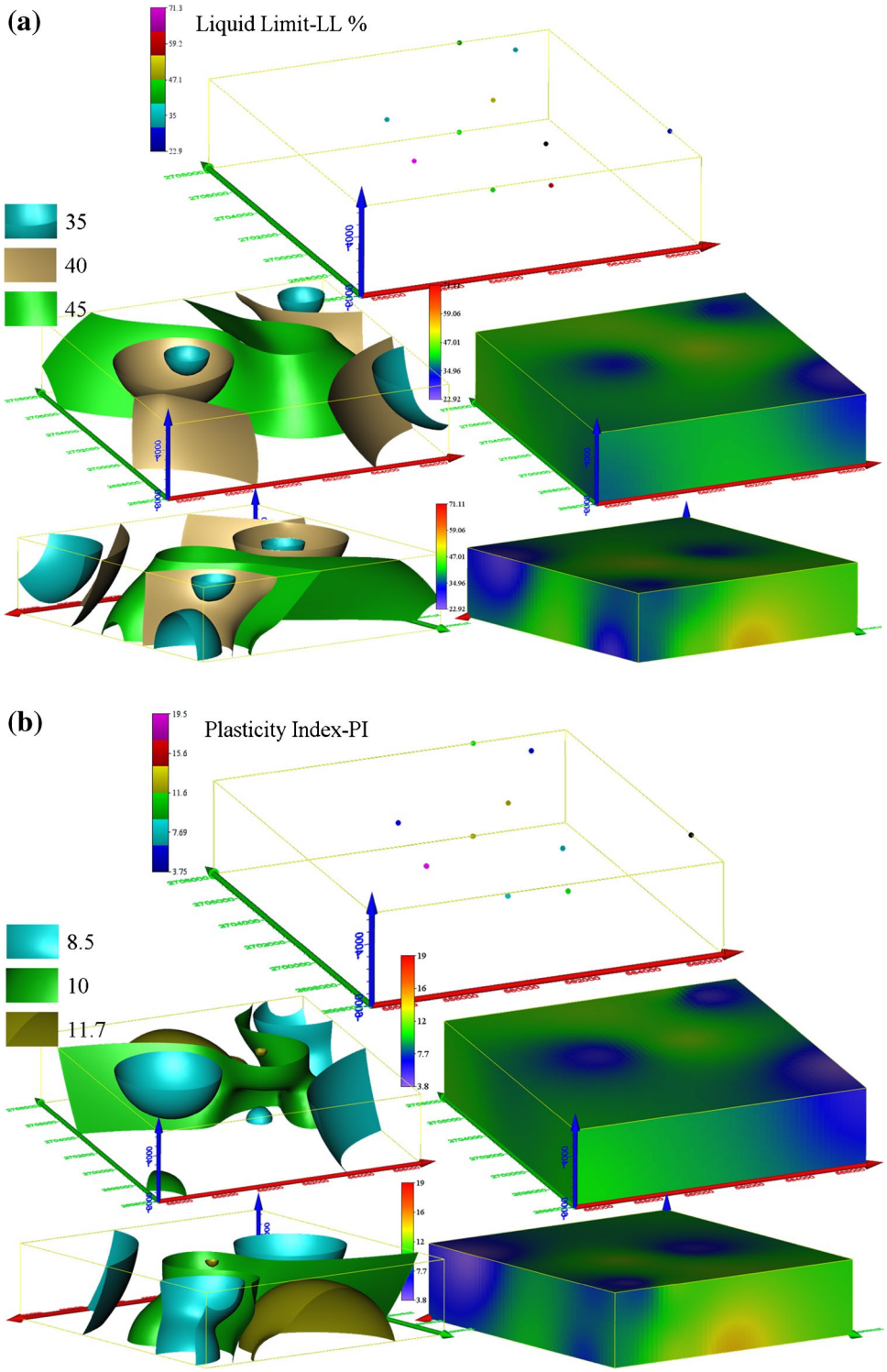

Fig. 6 Liquid limit (LL%) and plasticity index (PI)

The fill and the cohesive soils spread at shallow not exceeding 15 m depth. The swell potential of these soils clays, clayey silt, and silt is high and poses geotechnical problems accumulated east and west of Auhud mountain and north of Al-Manahil district. The cohessionless soils prevail on the surface at the periphery of the city and to a depth of more than 15 m elsewhere. Very dense to dense cohessionless soils predominate deep in the downtown area and change upward into medium dense to loose

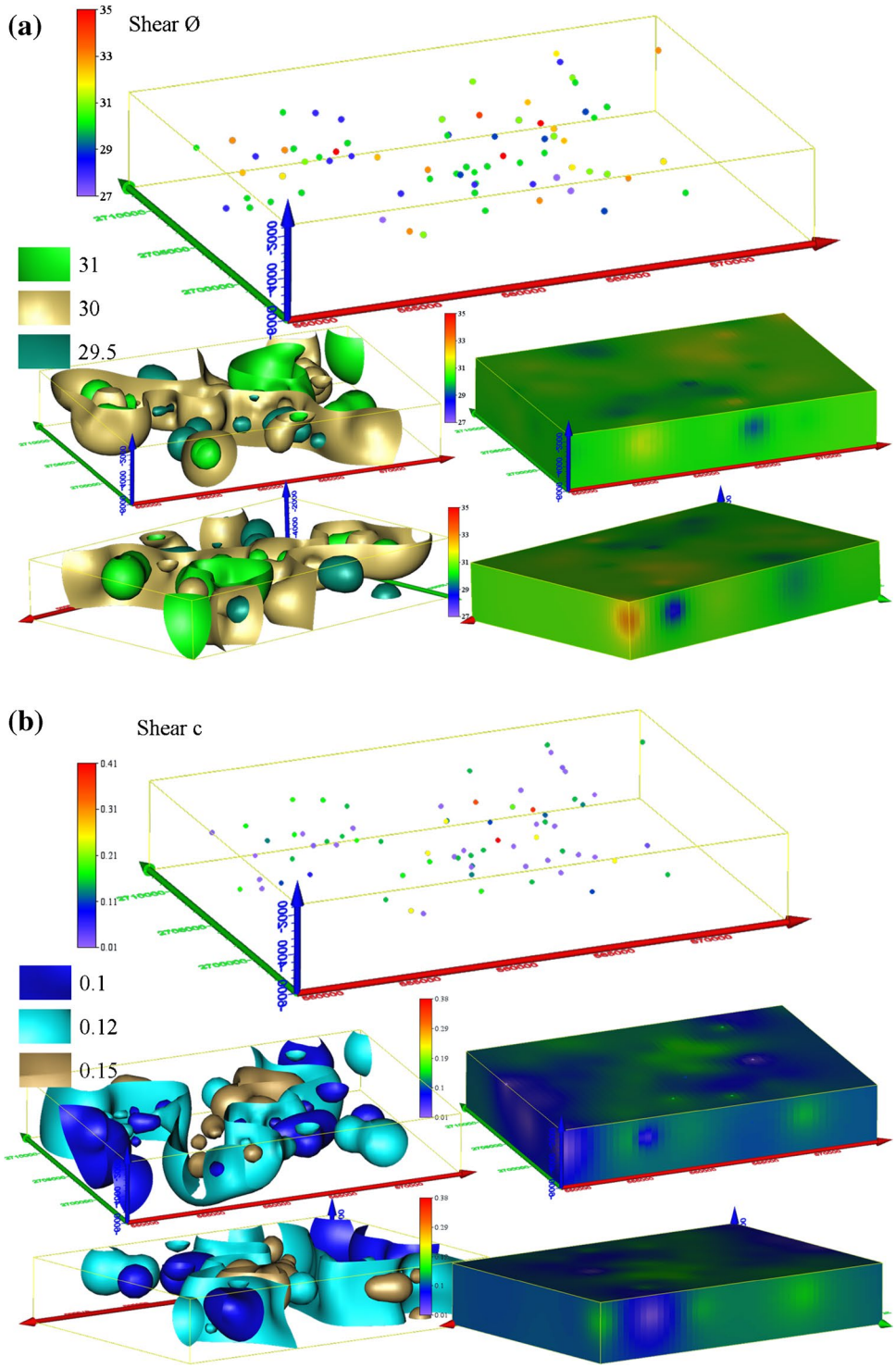

Fig. 7 Shear strength friction angle (Ø) and *c* index

varieties (Fig. 3b). Cohesive soils are recorded in 7 boreholes and varied from hard to soft (Fig. 3c).

Fill varied in thickness from 0.5 to 4.5 m that ranged from dense to loose. The fill layer of clayey sandy silt with gravel reaches maximum of 4.5 m in some parts of the Prophet's Holy Mosque area and decreases gradually to 1.5 m outward. Clay soils (1.5–6 m thick) were recorded in two boreholes and varied between loose cohessionless and stiff cohesive clays. Silts (0.5–7.5 m thick) were partly sandy, varied between loose to very dense cohessionless (14 samples) and soft to hard cohesive silts (17 samples). Sands (0.5–12.5 thick) were

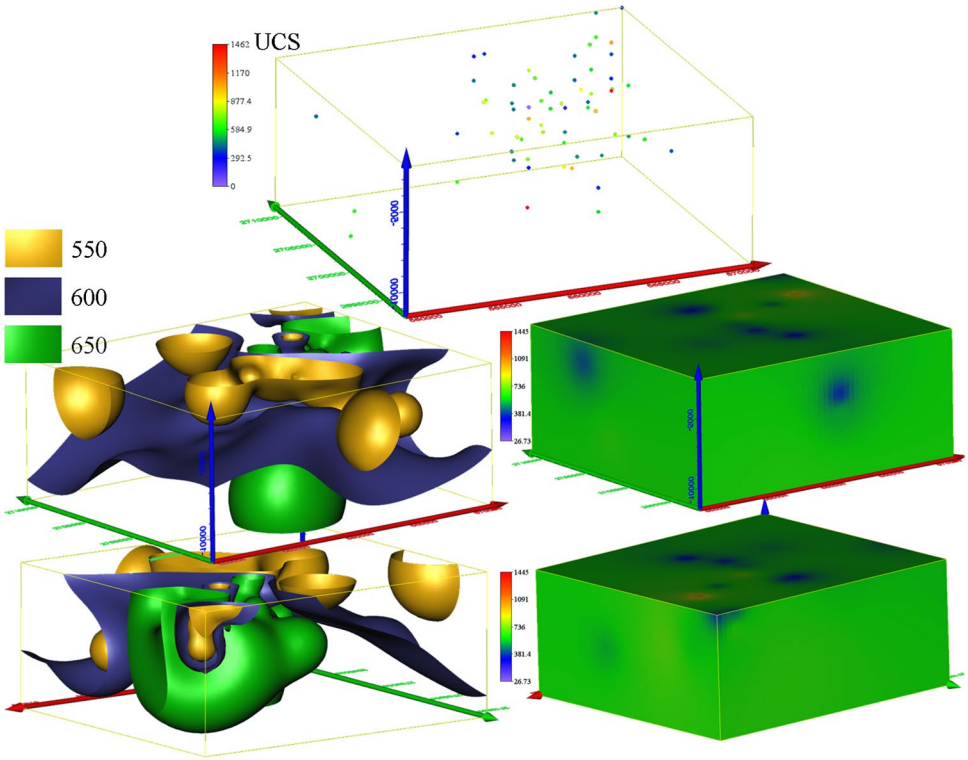

Fig. 8 Unconfined compression strength (UCS kg cm^{-2})

clayey to silty sand, and sand with silt, and gravel and/or cobbles ranged from medium to very dense cohessionless, plastic to non-plastic, and well to poorly graded (91 samples). Sand forms the top layer several meters thick over a wide area in the intermountain areas, west and along the foothills in the city, and decreases in thickness in the eastern area.

Gravels were sometimes silty to sandy, with silt, sand, and/or cobbles (0.5–8.5 m thick), medium to very dense cohessionless, plastic to non-plastic, and well to poorly graded (37 samples). Cobbles and boulders of vesicular basalt intermixed with sandy silt, silty sand, silty gravel, and gravel (0.5–10 m thick) of 10 samples proved very poor cohessionless. Cobbles and boulders commonly overlie the gravels in the city center that decrease in thickness and sometimes disappear at the peripheries. Sound bedrocks are represented mainly by vesicular basalt (33 boreholes) in the Harrat areas, rhyolite/granite (7 boreholes) close to the mountains, and andesite (1 boreholes) (Fig. 3d).

Basaltic vesicular lava (0.5 to 9 m thick) showed varying degrees of hardness, weathering, and fracturing and was excellent according to their RQD (69 samples). Rhyolite/granite bedrock (1–6 m thick) was excellent to very poor according to their corresponding RQD (14 samples). Andesite greenish grey bedrock of 1–1.5 m thick was recorded in one borehole and showed moderately hard, highly to intensely fractured, of poor to very poor RQD.

According to AASHTO classification (Fig. 4), 56.5% of soil samples showed A-1-b type, 19.5% A-2–4, 14% A-1-a, and 10% varied between A-7–5, A-4, A-2–6, A-3, and A-5. Soil types of A-1-b and A-2–4 dominate the area. A-1-b type consists of coarse-grained silty sand with gravel (50% 0.425 mm no. 40 and 25% 0.075 mm no. 200). A-2–4 type consists of coarse-grained silty clayey sand with gravel (35% 0.075 mm no. 200) with LL% < 40% and PI < 10.

Stochastic 3D geotechnical soil models

Grain size distribution varied in the 3D space (Fig. 5). Gravel reached 48% east of Ayr and Wairah mountains. Sand exceeded 60% in the wadi deposits west of Makhit and Kinana mountains. Fines have been maximum east and west of Uhud Mountain and in Al-Manahil district. Atterberg limits of LL and PI decrease upward at the southern boundary and reaches maximum in the area surrounding Auhud Mountain (Fig. 6).

Shear strength of soils is an important aspect to stability of shallow foundations and piles, slopes of dams and embankments, and lateral earth pressure on retaining walls. The most common laboratory methods employed to obtain shear strength parameters are direct shear test,

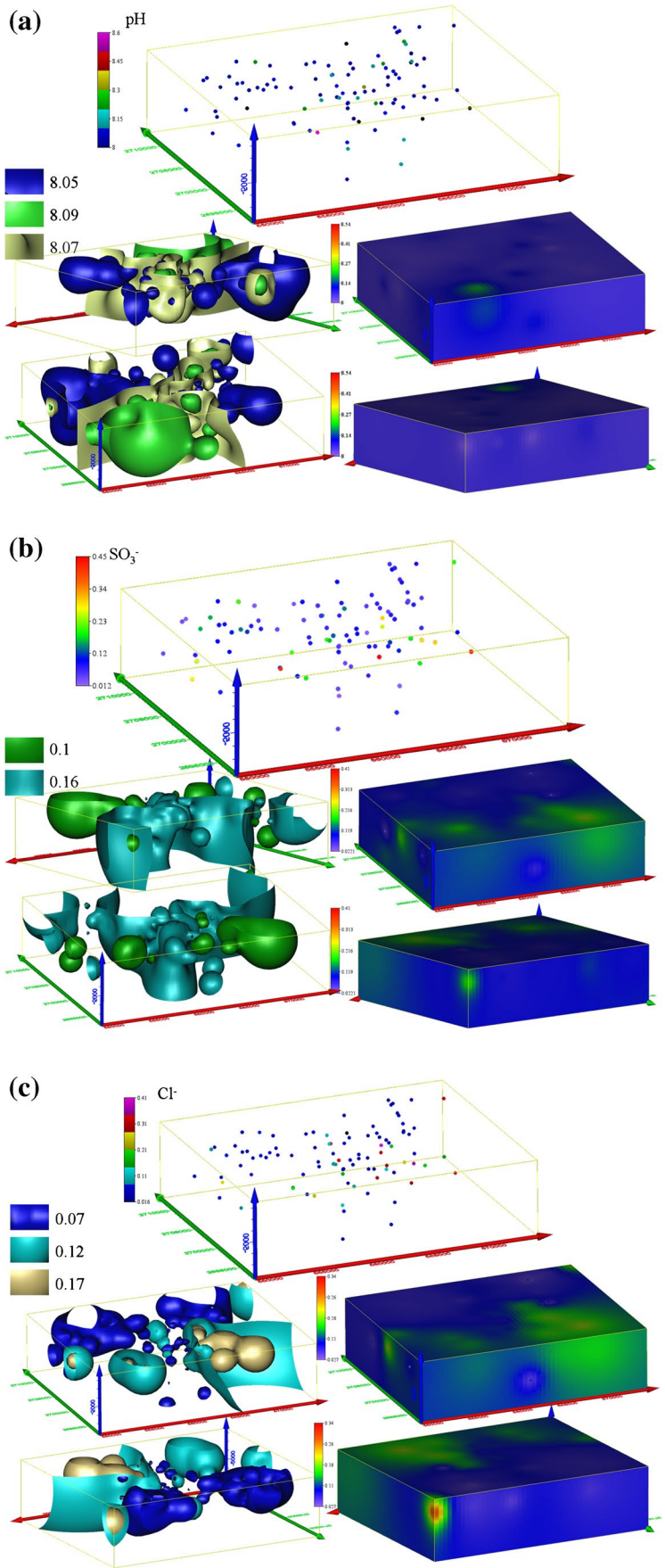

Fig. 9 Soil water **a** pH, **b** SO_3^-, and **c** Cl^-

tri-axial compression test, and unconfined compression test. The shear strength of cohessionless soils is affected by the internal friction: friction resistance to sliding and rolling of particles and interlocking. That is, estimated by the angle of internal friction, ϕ, and cohesion, c. Shear stress ϕ and c were largest in SW and NE (Fig. 7).

The unconfined compression strength showed largest values in the area surrounding Ayr Mountain and the northernmost occurrence of the Harrats (Fig. 8). Soil water chemistry 3D models are shown on Fig. 9. The pH clarified alkalinity with increase toward the south. Gradual southeastward increase of SO_3^- points to its possible source, the Harrat. Chlorides showed plumes east of Ayr Mountain and in the northern and western areas. Harrat is a major source of chloride and sulfates in the soil water. The high chloride and sulfate require protective measure for the reinforcement and concrete of the foundation.

Conclusions

The first insights from the 3D modeling of the geotechnical properties of soils in Medina proved potential in deciphering the complex subsurface for supporting subsoil future planning. It provides a future basis for integration with city master planning to ensure that the most efficient use of underground geo-assets is made to achieve optimal land sustainability. The methodology for building 3D models is now well established from the case study area that highlights their potential use in site appraisal before ground investigation and to identify underground resource potential based on the soil properties. The built models provide a relative assessment of ground suitability for safe construction based on sound assessment of their potential geotechnical properties and depth-related spatial zoning consistent with international standards and protocols. The geo-referenced database enhances the dynamicity of city-scale deterministic 3D models that can continuously be updated throughout all stages of development where the accuracy, scale, and resolution can be maximized by increasing the density of the borehole data.

The results of this research can enable city planners to prioritize areas with risks or over-costs for civil engineering projects. Specifically, the results can be used by geotechnicians, urban planners, or civil engineers for (a) evaluation and planning of urban areas according to the engineering conditions and the geohazard zones, (b) selection of engineering geological investigations areas of construction, (c) selection of a suitable foundation type and construction design, and (d) suppose changing of the engineering conditions and prediction of hazardous soil phenomena.

According to AASHTO classification, 90% of the soils were dominated by A-1-b (56.5%), A-2–4 (19.5%), and A-1-a (14%), and 10% varied between A-7–5, A-4, A-2–6, A-3, and A-5. Five main soil varieties were detected varied in grain sizes from clays to cobbles, sometimes overlain by dense to loose fills (0.5–4.5 m thick) and underlain, in some boreholes, by basalt, rhyolite/granite, or andesite.

Results are expected to foster future land-use optimization that identifies the most suitable soil use based on its geotechnical properties to support integrated and sustainable urban planning.

Acknowledgements The authors express their deepest gratitude for Prof Dr Abdullah M. Al-Amri, Editor-in-Chief of the Arabian Journal of Geosciences, and for the anonymous reviewers for their constructive comments which improved the quality of the manuscript.

Funding Open access funding provided by The Science, Technology & Innovation Funding Authority (STDF) in cooperation with The Egyptian Knowledge Bank (EKB).

Data availability Data is provided in the form of Voxler 3D models (Medina.voxb) in a compressed folder (3D Models.rar) upon request from the corresponding author.

References

Aldiss DT, Black MG, Entwisle DC, Page DP, Terrington RL (2012) Benefits of a 3D geological model for major tunnelling works: an example from Farringdon, east central London. UK Quart J Eng Geol Hydrogeol 45:405–414

Al-Shaibani AM, Lloyd JW, Abokhodair AA, Alahmari A (2007) Hydrogeological and quantitative groundwater assessment of the basaltic aquifer, Northern Harrat Rahat, Saudi Arabia. Arab Gulf J Sci Res 25:39–49

American Society for Testing and Materials Annual Book of ASTM Standards (ASTM), 2005. Vol. 04.08, Soil and Rock (I): D 420 –D 5611 and Vol. 04.09, Soil and Rock (II): D 5714-latest. West Conshohocken, Pennsylvania.

Camp, V.E., Roobol, M.J., 1991. Geologic map of cenozoic lava field of Harrat Rahat, Kingdom of Saudi Arabia, Directorate General of Mineral Resources, Geosciences Map GM-123, Scale 250,000 with text.

CGS, 2006. Canadian Foundation Manual, 4th Edition. The Canadian Geotechnical Society c/o BiTech Publisher Ltd.

Chang M, Chiu Y, Lin S, Ke T (2005) Preliminary study on the 2003 slope failure in Woo-wan-chai Area, Mt. Ali Road. Taiwan Eng Geol 80:93–114

Chrétien M, Fabre R, Denis A, Marache A (2007) Recherche des paramètres d'identification géotechnique optimaux pour une classification des sols sensibles au retrait gonflement. Rev Fr Géotech 120–121:91–106

Das, B.M., 2005. Fundamentals of geotechnical Engineering. 2nd Ed., Quebecor Printers.

De Rienzo F, Oreste P, Pelizza S (2008) Subsurface geological-geotechnical modelling to sustain underground civil planning. Eng Geol 96:187–204

Donghee K, Kyu-Sun K, Seongkwon K, Youngmin C, Woojin L (2012) Assessment of geotechnical variability of Songdo silty clay. Eng Geol 133–134:1–8

Hack R, Orlic B, Ozmutlu S, Zhu S, Rengers N (2006) Three and more dimensional modelling in geoengineering. Bull Eng Geo Environ 65:143–153

He H, He J, Xiao J, Zhou Y, Liu Y, Li C (2020) 3D geological modeling and engineering properties of shallow superficial deposits: a case study in Beijing, China. Tunn Undergr Sp Tech. 100, https://doi.org/10.1016/j.tust.2020.103390

Kolat Ç, Doyuran V, Can Ayday C, Lütfi Süzen M (2006) Preparation of a geotechnical microzonation model using Geographical Information Systems based on Multicriteria Decision Analysis. Eng Geol 87(3–4):241–255

Kolat Ç, Ulusay R, Lütfi Süzen M (2012) Development of geotechnical microzonation model for Yenisehir (Bursa, Turkey) located at a seismically active region. Eng Geol 127:36–53

Masoud AA (2015) Geotechnical evaluation of the alluvial soils for urban land management zonation in Gharbiya governorate. Egypt J Afr Earth Sci 101:360–374

Masoud AA, Kamh SZ, Elgharib SR (2016) Subsurface geological-geotechnical 3D modeling to evaluate the geohazard of the alluvial soils in Tanta Region. Egypt GIS Approach Delta J Sci 37:117–127

Pellaton, C. 1981. Geologic map of the Al Medinah Quadrangle, Sheet 24D, Kingdom of Saudi Arabia Deputy Ministry for Mineral Resources Geologic Map GM-52C,Scale 250,000, with text.

Phien-wej N, Giao PH, Nutalaya P (2006) Land subsidence in Bangkok. Thailand Eng Geol 82:187–201

Price SJ, Terrington RL, Busby J, Bricker S, Berry T (2018) 3D ground-use optimisation for sustainable urban development planning: a case-study from Earls Court, London. UK Tunn Undergr Sp Tech 81:144–164

Scott, R.F., 1963. Principles of soil mechanics. Reading, Mass., Addison-Wesley Publishing Co., Inc.

Okasha TM, Abduljauwad SN (1992) Expansive soil in Al-Medinah. Saudi Arabia Appl Clay Sci 7(4):271–289